Available online at www.sciencedirect.com
ScienceDirect
Journal of Molecular Catalysis B: Enzymatic 50 (2008) 128–140
JOURNAL OF MOLECULAR CATALYSIS B: ENZYMATIC
www.elsevier.com/locate/molcatb

Characterization of recombinant fusion constructs of human β1,4-galactosyltransferase 1 and the lipase pre-propeptide from *Staphylococcus hyicus*

B. Sauerzapfe [a], D.-J. Namdjou [a], T. Schumacher [a], N. Linden [a], K. Křenek [b], V. Křen [b], L. Elling [a,*]

[a] *Laboratory for Biomaterials, Institute of Biotechnology and Helmholtz-Institute for Biomedical Engineering, RWTH Aachen University, Worringer Weg 1, D-52074 Aachen, Germany*
[b] *Institute of Microbiology, Centre of Biocatalysis and Biotransformation, Academy of Sciences of the Czech Republic, Videnska 1083, 142 20 Prague 4, Czech Republic*

Available online 11 September 2007

Abstract

The question whether proteins fused to β1,4galactosyltransferase (β4GalT-1) influence the biocatalytic properties of the glycosyltransferase has not been addressed so far. In the present study we have chosen a novel approach to express the gene encoding for human β4GalT-1 from placenta in an N-terminal fusion with the pre-propeptide of the lipase from *Staphylococcus hyicus*. The pre-propeptide provides a secretion signal in *Escherichia coli* and was reported to protect fused proteins against proteolytic degradation. Expression of the fusion protein was challenged with an almost full-length version of human β4GalT-1 including parts of the signal anchor and the stem region (propeptide-natβ4GalT-1) and the full catalytic domain (His_6propeptide-catβ4GalT-1), respectively. We demonstrate that the fusion protein in propeptide-natβ4GalT-1 is cleaved off during purification using immobilized metal ion chromatography IMAC, most probably catalyzed by the immobilized Zn^{2+} ions. Cleavage can be avoided by deletion of five C-terminal amino acids of the propeptide and the stem region yielding His_6propeptide-catβ4GalT-1. Kinetic data reveal that both enzyme constructs possess specific biocatalytic characteristics when compared to a recombinant luminal β4GalT-1 construct. The catalytic efficiency towards more hydrophobic acceptor glycosides, e.g. benzyl 2-acetamido-2-deoxy-β-D-glucopyranoside and *p*-nitro phenyl 2-acetamido-2-deoxy-β-D-glucopyranoside, and the *N*-glycans of IgG from rat is significantly increased. In summary, the His_6propeptide-catβ4GalT-1 is very useful for biocatalytic applications involving hydrophobic acceptor glycosides and the propeptide-natβ4GalT-1 is able to glycosylate glycoproteins in an efficient way.

Keywords: Human β1,4-galactosyltransferase; Fusion protein; Lipase propeptide; *Staphylococcus hyicus*; Hydrophobic acceptor substrates

1. Introduction

β1,4-Galactosyltransferase 1 (EC 2.4.1.38, β4GalT-1) is the best characterized Leloir-glycosyltransferase in glycobiology. Together with six other members it belongs to the homologous β4GalT family [1,2] in the CAZY family 7 of inverting glycosyltransferases (http://afmb.cnrs-mrs.fr/CAZY/). Many papers have elucidated different aspects on β4GalT-1 concerning the genetics [3], the biochemistry, and cell biology [4], as well as its 3D-structure [5–8]. β4GalT-1 is known to transfer D-galactose in the presence of manganese as a cofactor from UDP-galactose to *N*-acetylglucosamine to form *N*-acetyllactosamine (Galβ1-4GlcNAcβ1-R, LacNAc type 2) (Scheme 1A). Together with α-lactalbumin β4GalT-1 constitutes the lactose synthase (EC 2.4.1.22) which specifically synthesizes lactose. As a type II transmembrane glycoprotein β4GalT-1 is a *trans*-Golgi resident enzyme with a short N-terminal cytoplasmic sequence, a transmembrane anchor, a short stem region, and a large C-terminal catalytic domain (Scheme 2) [9–11]. Soluble forms of the mammalian enzyme can be found in several body fluids, e.g. typically in serum and milk due to proteolytic cleavage sites in the stem region.

Since LacNAc (type 2) is a basic structural element of terminal carbohydrate ligands ($Lewis^x$, $Lewis^y$, blood groups) and

* Corresponding author. Tel.: +49 241 8028350; fax: +49 241 8022387.
E-mail address: L.Elling@biotec.rwth-aachen.de (L. Elling).

1381-1177/$ – see front matter © 2007 Elsevier B.V. All rights reserved.
doi:10.1016/j.molcatb.2007.09.009

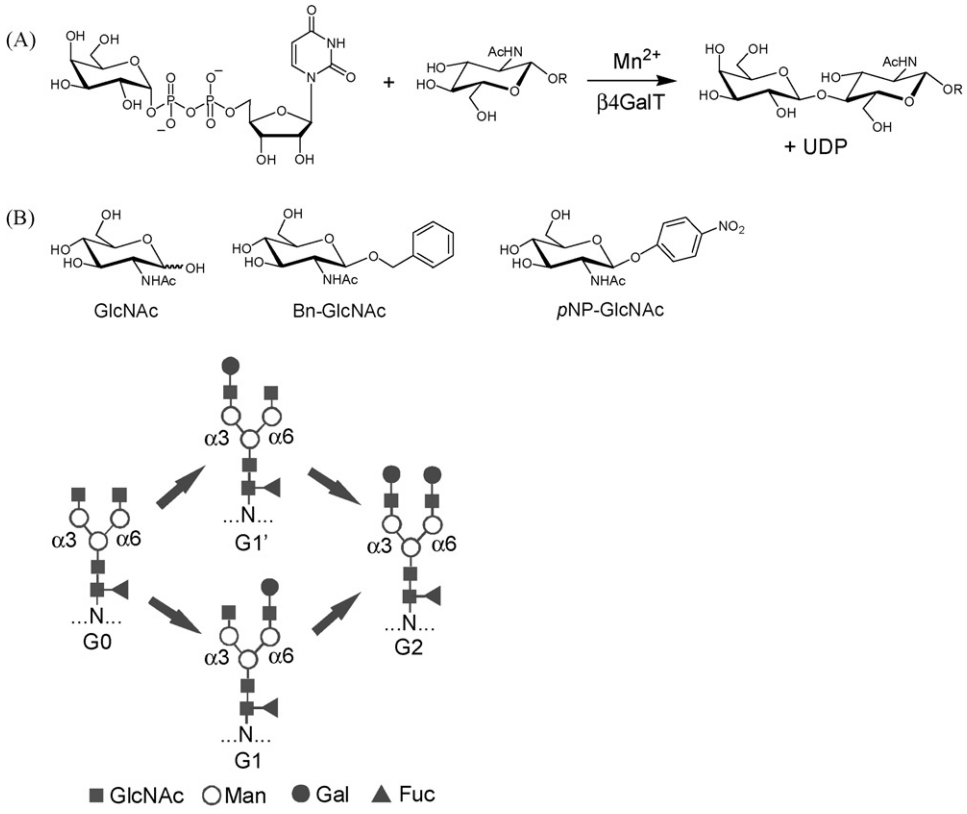

Scheme 1. Reaction of β1,4-galactosyltransferase constructs (A) using the acceptor substrates (B) GlcNAc, benzyl 2-acetamido-2-deoxy-β-D-glucopyranoside (Bn-GlcNAc), and *p*-nitrophenyl 2-acetamido-2-deoxy-β-D-glucopyranoside (*p*NP-GlcNAc). Additionally, rat IgG was tested as acceptor substrate.

poly-LacNAc in glycoproteins and lipids the *in vitro* synthesis of LacNAc-containing (neo)glycoconjugates is still highly interesting for screening carbohydrate–protein interactions. β4GalT preparations from bovine or human milk were employed in biocatalytic *in vitro* processes yielding LacNAc and derivatives thereof [12–15]. The *in vitro* synthesis of LacNAc derivatives was pushed using recombinant β4GalT-1 in combination with the development of efficient microbial expression systems [16–19]. Strategies for the expression of soluble human β4GalT-1 in *Escherichia coli* were aimed at minimizing the formation of inclusion bodies [18] and secretion into the oxidizing environment of the periplasm because of a single disulfide bond

```
Bov.   1  MKFREPLLGGSAAMPGASLQRACRLLVAVCALHLGVTLVYYLAGRDLRRLPQLVGVHPPL
Hum.   1  MRLREPLLSG-AAMPGASLQRACRLLVAVCALHLGVTLVYYLAGRDLSRLPQLVGVSTPL
          *  ***** * ************************************ ********  **
Bov.  61  QGSSHGAAAIGQPSGELRLRGVAPPPPLQNSSKPRSRAPSNLDAYSHPGPGPGPGSNLTS
Hum.  60  QGGSNSAAAIGQSSGELRTGGARPPPPLGASSQPRPGGDSSPVVDS----GPGPASNLTS
          ** *  ****** *****  *  *****  ** **    *     *    **** *****
Bov. 121  APVPSTTTRSLTACPEESPLLVGPMLIEFNIPVDLKLIEQQNPKVKLGGRYTPMDCISPH
Hum. 116  VPVPHTTALSLPACPEESPLLVGPMLIEFNMPVDLELVAKQNPNVKMGGRYAPRDCVSPH
           *** ** ********************** **** *   *** ** **** * ** ***
Bov. 181  KVAIIILFRNRQEHLKYWLYYLHPILQRQQLDYGIYVINQAGESMFNRAKLLNVGFKEAL
Hum. 176  KVAIIIPFRNRQEHLKYWLYYLHPVLQRQQLDYGIYVINQAGDTIFNRAKLLNVGFQEAL
          ****** ***************** *****************   ************ ***
Bov. 241  KDYDYNCFVFSDVDLIPMNDHNTYRCFSQPRHISVAMDKFGFSLPYVQYFGGVSALSKQQ
Hum. 236  KDYDYTCFVFSDVDLIPMNDHNAYRCFSQPRHISVAMDKFGFSLPYVQYFGGVSALSKQQ
          ***** ***************** ************************************
Bov. 301  FLSINGFPNNYWGWGGEDDDIYNRLAFRGMSVSRPNAVIGKCRMIRHSRDKKNEPNPQRF
Hum. 296  FLTINGFPNNYWGWGGEDDDIFNRLVFRGMSISRPNAVVGRCRMIRHSRDKKNEPNPQRF
          ** ****************** *** ***** ****** * ********************
Bov. 361  DRIAHTKETMLSDGLNSLTYMVLEVQRYPLYTKITVDIGTPS
Hum. 356  DRIAHTKETMLSDGLNSLTYQVLDVQRYPLYTQITVDIGTPS
          ******************** ** ******** *********
```

Scheme 2. Alignment of bovine β4GalT-1 (P08037 with 402 amino acids, GenBank accession number X14558) and human β4GalT-1 (from human placenta, P15291 (minus S11) with 397 amino acids, GenBank accession number X14085) [11,52]. LLVAVCAL. . .: transmembrane domain; RDLRRLP. . .: start of lumenal region and stem region; S start of the minimal catalytic domain. The human enzyme was used in this study.

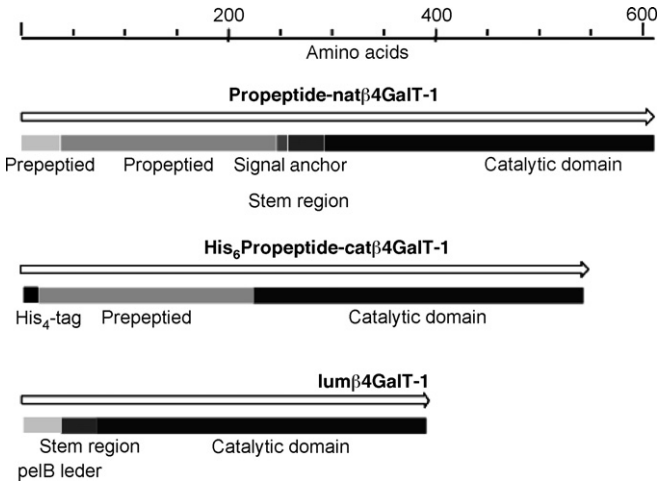

Scheme 3. Enzyme constructs used in this study. The propeptide-natβ4GalT-1 and the lumβ4GalT-1 are secreted into the periplasm of *Escherichia coli*, by which the pre-peptide secretion signal (38 amino acids, light grey) of the lipase from *Staphylococcus hyicus* and the pelB leader sequence (23 amino acids, light grey) are cleaved off. The His_6propeptide-catβ4GalT-1 is expressed in the cytoplasm of *E. coli*. Propeptide-natβ4GalT-1: propeptide sequence (207 amino acids, dark grey) of the lipase from *S. hyicus*. The human β4GalT-1 sequence starts with 11 amino acids of the signal anchor sequence (underlined), followed by the stem region (33 amino acids) and the catalytic domain (321 amino acids, in bold black). His_6propeptide-catβ4GalT-1: propeptide sequence deleted by C-terminal DKKPY (202 amino acids) and 323 C-terminal amino acids of human β4GalT-1 including the catalytic domain. lumβ4GalT-1: 354 C-terminal amino acids of human β4GalT-1 including the 32 amino acids of the stem region and catalytic domain.

important for activity [20–22]. On the other hand, the production of inclusion bodies was optimized for subsequent refolding of active bovine β4GalT-1 [16,23]. Expression of recombinant human β4GalT-1 in *Saccharomyces cerevisiae* or *Pichia pastoris* had to be optimized with respect to secretion into the culture medium and minimizing hyperglycosylation for binding of the His-tagged enzyme [17,24,25]. So far, the highest specific activities for recombinant human β4GalT-1 were reported to be 15 mU/mg for secretion by *P. pastoris* [24] and 87 mU/mg for secretion of a maltose-binding-protein (MBP) fusion protein by *E. coli* [22]. The latter was characterized after cleaving off the MBP fusion protein.

Biocatalytic applications employing the recombinant catalytic domain of bovine and human β4GalT-1 (Scheme 2) resulted in a range neoglycoconjugates by the use of non-natural donor or acceptor substrates [26,27]. Due to the high homology of the catalytic domains differences in the biocatalytic properties of both enzymes were not described and are not expected. However, the question whether an intact fusion protein of β4GalT-1 provides a glycosyltransferase with distinct properties has not been addressed.

In the present study we have chosen a novel approach to express the gene encoding for human β4GalT-1 from placenta. The N-terminal fusion with the pre-propeptide (245 amino acids) of the lipase from *S. hyicus* (Scheme 3) provides the short N-terminal hydrophilic pre-peptide (38 amino acids) followed by a long hydrophobic propeptide (207 amino acids) [28]. The pre-propeptide was previously used for secretion of heterologous proteins in gram-positive bacteria [29] because of its protection of the fused target proteins against proteolytic degradation. In addition, the pre-peptide represents a secretion signal in *E. coli* [30] giving periplasmic expression.

In contrast to other strategies where the production of the minimal catalytic domain of β4GalT-1 in *E. coli* was optimized, our first experiment challenged the expression of the almost full-length gene of human β4GalT-1 in order to determine the biocatalytic properties of the resulting enzyme construct. The full length β4GalT-1 from human placenta [11] (Scheme 2) deleted by 32 N-terminal amino acids was fused at the N-terminus with the pre-propeptide (Scheme 3). This novel construct is expressed in the periplasm of *E. coli* as soluble protein. We report here on the properties of the propeptide construct of β4GalT-1 during IMAC purification and its kinetic characteristics. These investigations led us further to a fusion construct of the propeptide with the catalytic domain of β4GalT-1 alone yielding soluble expression of human β4GalT-1 in the cytoplasm of *E. coli*. By comparison with the luminal β4GalT-1 actively expressed in the periplasm of *E. coli* we further demonstrate that both fusion constructs exhibit distinct biocatalytic properties towards different monosaccharide acceptor substrates (Scheme 1B) and IgG as glycoprotein.

2. Materials and methods

2.1. General methods

PCR reactions were performed using Taq-Polymerase from Eppendorf® (Hamburg, Germany). PCR Products and plasmids were purified by "MinElute Kits", "Plasmid Purification Kit" (QIAGEN®, Hilden, Germany), "Wizard® SV Gel", and the "PCR Clean-Up System" from Promega® (Mannheim, Germany). Restriction enzymes, alkaline phosphatase (Shrimps), and the "Rapid DNA Ligation Kit" were from Roche® (Basel, Switzerland). The integrity of all gene constructs was confirmed by sequencing (Sequiserve, Vaterstetten, Germany).

3. Synthesis of *p*-nitrophenyl 2-acetamido-2-deoxy-β-D-glucopyranoside (*p*NP-GlcNAc)

2-Acetamido-3,4,6-tri-*O*-acetyl-2-deoxy-α-D-glucopyranosyl chloride [31,32].

A suspension of 2-acetamido-2-deoxy-D-glucose (25 g, 0.113 mmol) in acetyl chloride (50 mL) and CH_2Cl_2 (100 mL) was stirred overnight. The reaction mixture was diluted with further portion of CH_2Cl_2 (100 mL) and poured onto water–ice mixture. The organic phase was extracted with ice-cold saturated aqueous solution of $NaHCO_3$ (2× 150 mL) and with ice-cold water (150 mL). The organic phase was dried (Na_2SO_4), concentrated and precipitated with rapid addition of dry diethyl ether (200 mL). After 4 h a white crystalline precipitate was filtered off, washed with dry ether and shortly dried on air yielding the title compound (33 g, 80%). The NMR spectra were in compliance with literature [33].

p-Nitrophenyl 2-acetamido-3,4,6-tri-*O*-acetyl-2-deoxy-β-D-glucopyranoside [34].

A solution of 2-acetamido-3,4,6-tri-*O*-acetyl-2-deoxy-α-D-glucopyranosyl chloride (3.51 g, 9.6 mmol), tetrabutylammonium hydrogen sulfate (3.27 g, 9.6 mmol), and *p*-nitrophenol (2.67 g, 19.2 mmol) in a mixture of CH_2Cl_2 (35 mL) and 1 M NaOH (35 mL) was stirred vigorously for 1 h. The mixture was extracted with CH_2Cl_2 (4× 75 mL), and washed with 1 M NaOH (4× 200 mL) and water (until the yellow colour disappeared). Combined organic phases were dried (Na_2SO_4) and evaporated *in vacuo*. The residue was crystallised from MeOH/EtOAc to give title compound (3.4 g, 76%). The NMR spectra were in compliance with literature [35].

p-Nitrophenyl 2-acetamido-2-deoxy-β-D-glucopyranoside [34].

The above *p*-nitrophenyl 2-acetamido-3,4,6-tri-*O*-acetyl-2-deoxy-β-D-glucopyranoside (2.45 g, 5.2 mmol) was suspended in dry MeOH (70 mL). Methanolic solution of NaOMe (1 M, 2.5 mL) was added and the mixture was stirred until dissolution was complete (5 min). Dowex 50WX2-200 (5 g, previously washed in methanol) was added and after 1 min removed by filtration. The solution was evaporated *in vacuo* to dryness. White solid was recrystallised from water and suspended in acetone (50 mL). The mixture was stirred for 30 min, and the product was filtered off and dried to give the title compound as white solid (1.68 g, 94%). The NMR spectra were in compliance with literature [36].

3.1. Strains

E. coli NovaBlue *endA1 hsdR17* ($r_{K12}^{-}m_{K12}^{+}$) *supE44 thi-1 recA1 gyrA96 relA1 lac* F′[*proA*$^+$*B*$^+$ *lacI*^{q}*ZΔM 15*:Tn*10* (Tc^R)] (Novagen, Darmstadt, Germany) was used for propagation of plasmids. *E. coli* BL21(DE3) F^- *ompT hsdS*$_B$($r_B^-m_B^-$) *gal dcm* (DE3) was used for the expression of the described β4GalT-1 constructs (Novagen, Darmstadt, Germany).

3.2. Cloning of the β4GalT-1 constructs

3.2.1. Pre-propeptide-natβ4GalT-1

The expression vector pLGalTΔ38 was kindly provided by Prof. Dr. R. Freudl and Dr. M. Klein (Institute of Biotechnology 1, Research Centre Jülich, Germany). Therefore the gene encoding human β4GalT-1 from placenta (GenBank accession number X14085) was cut StyI and ligated with the StyI cut pUC18 plasmid via blunt end ligation. The resulting vector was pGalTΔ38. The following step comprised the restriction of the pUC18 derivative pI183K23 SnaBI/HindIII which contained the lipase gene under the control of the *lacZ* promoter. The restriction product contained the plasmid (pI183K23) with the pre-propeptide of the lipase cut SnaBI/HindIII under the control of the *lacZ* promoter. This plasmid was ligated via blunt end ligation with the StyI/HindIII cut pGalT38, resulting the coding sequence of human β4GalT-1 from placenta deleted by the first 32 amino acids. The finally resulting plasmid pLGalTΔ38 is a derivative of pUC18 [30] and contains the coding sequence of human β4GalT-1 from placenta (Swiss-Prot data bank P15291) deleted by the first 32 amino acids and leaving 11 amino acids of the transmembrane anchor. The N-terminal fusion with the pre-propeptide sequence of the lipase from *S. hyicus* results in the pre-propeptide-nativeβ4GalT-1 (pre-propeptide-natβ4GalT-1) consisting of 38 amino acids for the pre-peptide, 207 amino acids for the propeptide, 11 amino acids signal anchor of human β4GalT-1, 33 amino acids of the stem region, and 321 amino acids of the catalytic domain (Scheme 3). The stem region and the catalytic domain constitute the luminal part of human β4GalT-1 (Scheme 2). The fusion protein (610 amino acids) is under the control of the *lacZ* promoter with ampicillin resistance as selection marker. The pre-peptide mediates secretion into the periplasm of *E. coli* [30] and is cleaved off. The resulting product is designated propeptide-natβ4GalT-1 and consists of 572 amino acids.

3.2.2. His_6propeptide-catβ4GalT-1

Site-specific PCR mutagenesis [37] was used to create the restriction sites MunI and XhoI for the insertion of the catalytic domain of the β4galT-1 gene into the expression vector pET16b (Novagen, Darmstadt, Germany). The vector pLGalTΔ38 was chosen as template using the two primers 5′-GTC*CAATTG*GCTCGCTTGTGATGTAAATTT-3′ and 3′-CCG*CTCGAG*CGGCTAGCTCGGTGTCCCGATGTCCACTGTGATTTGGGTATA-5′ for PCR amplification of the catalytic domain. Therefore the Taq DNA Polymerase from Eppendorf® was used following the standard protocol. In order to fuse the propeptide sequence (207 amino acids deleted by five C-terminal amino acids) of the lipase of *S. hyicus* with the catalytic domain site-specific PCR mutagenesis was used to create the restriction sites NcoI and MunI for cloning of the propeptide sequence. The existing vector pLGalTΔ38 was chosen as template for PCR amplification using the two primers 5′-CATG*CCATGG*GCCATCATCATCATCATCATAATGATTCGACAACACAAACAACGACACCACTGGAAGTCGCTCAAACGTCGCAG-3′ and 3′-CTC*CAATTG*CGGACCGGAGGGGCCCGGCC-5′. The PCR fragments coding for the propeptide and catalytic domain were digested by NcoI/MunI or MunI/XhoI, respectively, and ligated with NcoI/XhoI digested pET16b vector) using the rapid DNA ligation kit from Roche. The resulting expression vector pTS05 produce His_6propeptide-catβ4GalT-1 (533 amino acids including 323 amino acids of β4GalT-1) in the cytoplasm of *E. coli* after induction by IPTG (Scheme 3).

3.2.3. Lumβ4GalT-1

Site-specific PCR mutagenesis [37] was used to create the restriction sites NcoI and XhoI for the insertion of the luminal part of β*4*galT-1 gene into the expression vector pET22b. The existing vector pLGalTΔ38 was chosen as template using the two primers 5′-CATG*CCATGG*ACCTGAGCCGCCTGCCCCAACTGGTC-3′ and 3′-CCG*CTCGAG*CGGCTAGCTCGGTGTCCCGATGTCCACTGTGATTTGGGTATA-5′ for PCR amplification. Therefore the Taq DNA Polymerase from Eppendorf® was used following the standard protocol. The PCR fragment was digested by NcoI/XhoI and ligated with NcoI/XhoI digested pET22b vector (Novagen, Darmstadt, Ger-

many) using the rapid DNA ligation kit from Roche. The resulting vector plumβ4GalT-1 provides expression of the luminal β4GalT-1 (lumβ4GalT-1, 354 amino acids) into the periplasm of *E. coli* (Scheme 3).

3.3. Production and purification of β4GalT-1 constructs

3.3.1. Pre-propeptide-natβ4GalT-1

Transformants were grown in 100 mL Erlenmeyer flasks containing 20 mL LB-medium with 100 μg/mL ampicillin. The cultures were incubated overnight at 37 °C and 130 rpm. For protein production cells were grown in 5 L Erlenmeyer flasks with 1 L LB-medium containing 100 μg/mL ampicillin. After 20 h incubation at 37 °C (OD_{600} = 0.5–0.6) and 75 rpm 500 μL of 1 M isopropyl thiogalactoside (IPTG) was added for a final concentration of 0.5 mM. The cells were harvested after 2 h by centrifugation. A 20% (w/w) cell suspension in 100 mM HEPES–NaOH buffer pH 8 was disrupted by sonication and the supernatant was used for further purification after centrifugation. A two-step procedure with anion exchange chromatography (IEX) using Q-sepharose fast flow (Pharmacia, Uppsala, Sweden) as the first step was applied for purification of propeptide-natβ4GalT-1 from the crude extract. The crude extract was loaded onto a column (2.6 cm × 20 cm, 5 mL/min), which was previously equilibrated with 500 mL 50 mM HEPES–NaOH, pH 8. Propeptide-natβ4GalT-1 did not bind and was collected for the second purification step with IMAC using Zn^{2+}-NTA columns (Qiagen, Hilden, Germany). The protein fraction from the IEX was loaded onto a column (2.6 cm × 10 cm, 5 mL/min) which was previously equilibrated with 300 mL, 100 mM HEPES–NaOH, pH 8. After a washing step with the same buffer 25 mM imidazole was added to the buffer for elution. All fractions were analysed for their protein concentration [38] and assayed for β4GalT-1 activity.

3.3.2. His_6propeptide-catβ4GalT1

Transformants were grown as described above. Cells were grown in 5 L Erlenmeyer flasks with 1 L TB-medium containing 0.1 mM IPTG and 100 μg/mL ampicillin. After 20 h incubation at 25 °C and 75 rpm the cells were harvested by centrifugation. A 40% (w/w) cell suspension in 50 mM HEPES–NaOH, 0.3 M NaCl, 10 mM imidazole pH 8 was disrupted by sonication and the supernatant was used for the further purification after centrifugation. IMAC using Ni^{2+}-NTA columns (Qiagen, Hilden, Germany) was applied for the purification of the His_6propeptide-catβ4GalT1 directly from the crude extract. *E. coli* crude extract (30 mL) was loaded onto a column (1.6 cm × 10 cm, 1.5 mL/min), which was previously equilibrated with 200 mL 50 mM HEPES–NaOH, 0.3 M NaCl, 10 mM imidazole pH 8. After a washing step with 50 mM HEPES–NaOH, 0.3 M NaCl, 20 mM imidazole pH 8 the concentration of imidazole was raised to 250 mM for elution. All fractions were analysed as described before.

3.3.3. Lumβ4GalT-1

Transformants were grown as described above. Cells were grown in 5 L Erlenmeyer flasks with 1 L LB-medium containing 0.05 mM IPTG and 100 μg/mL ampicillin. After 20 h incubation at 25 °C and 75 rpm the cells were harvested by centrifugation. A 30% (w/w) cell suspension in 100 mM HEPES–NaOH buffer pH 8 was disrupted by sonication and the supernatant was used for the further purification after centrifugation. Cation exchange chromatography using SP-sepharose fast flow (Pharmacia, Uppsala, Sweden) was applied for the purification of the lumβ4GalT1 directly from the crude extract. *E. coli* crude extract was loaded onto a column (2.6 cm × 9.2 cm, 5 mL/min) which was previously equilibrated with 300 mL 50 mM HEPES–NaOH, pH 7. After a washing step with the same buffer the elution was carried out using 50 mM HEPES–NaOH, 1 M NaCl, pH 7. The eluted fractions were analysed as described above.

3.4. Activity assays

The activities of β4GalT-1 constructs were determined by a photometric assay and a HPLC assay. The photometric assay was performed according to the method described by Barratt et al. [39] using the pyruvate kinase/lactate dehydrogenase system for the detection of produced UDP. The microtiter plate assay contained 100 mM HEPES–NaOH, pH 8, 20 mM KCl, 2 mM K_2HPO_4, 4 mM $MgCl_2$, 1 mM phosphoenolpyruvate, 0.25 mM NADH, 10 mM benzyl 2-acetamido-2-deoxy-β-D-glucopyranoside (Bn-GlcNAc), 2 mM UDP-Gal, 3 mM $MnCl_2$, 5 U pyruvate kinase, and 5 U lactate dehydrogenase in a total volume of 250 μL. The reaction was started by addition of 100 μL enzyme solution and followed at 340 nm at 37 °C. Control experiments for the detection of side activities were done without donor or acceptor substrate.

Enzyme activity was also determined by HPLC detection of LacNAc. The assay solution contained 2.5 mM UDP-Gal, 25 mM GlcNAc in 100 mM HEPES–NaOH pH 8 with 1 mM $MnCl_2$ and was incubated at 37 °C after addition of enzyme solution. The reaction was stopped at different time points where the conversion rate was linear by heating for 5 min at 95 °C. The centrifuged samples were analysed by HPLC on a Aminex® Ion Exclusion HPX87H column (300 mm × 7.8 mm, Bio-Rad, München, Germany) and elution with 5 mM H_2SO_4 at 65 °C (flow rate 0.5 mL/min, 20 μL sample volume, detection at 205 nm and 254 nm). The concentration of formed LacNAc was determined by a standard calibration curve and used for subsequent calculation of enzyme units.

For both assays 1 U of β4GalT-1 is the amount of enzyme producing 1 μmol product (UDP or LacNAc) per minute.

3.5. SDS-PAGE and western blot

SDS-PAGE analysis of reduced samples was performed with 10–12% precast Bis-Tris NuPAGE®/Nowex®-gel applying the standard protocol with MOPS as running buffer (Invitrogen, Paisley, UK). Samples were diluted and 20 μg protein was loaded onto each slot of the gel. A pre-mixed protein standard was used for the determination of the molecular mass. The protein gels were stained with Coomassie blue.

Table 1
Purification of propeptide-natβ4GalT-1, lumβ4GalT-1 and His_6propeptide-β4GalT-1

	Volume (mL)	Total activity (mU)	Protein amount (mg)	Specific activity (mU/mg)	Purification factor (–)	Yield (%)
(A) Propeptide-natβ4GalT-1 (3.5 g wet cell mass from 1 L culture)						
Crude extract	14	5287	198.8	27	1	100
IEX Q-sepharose	80	4600	28.0	163	6	87
IMAC Zn^{2+}-NTA	20	2622	5.6	468	17	50
(B) His_6propeptide-β4GalT-1 (11.5 g wet cell mass from 1 L culture)						
Crude extract	34	1466	676.6	2	1	100
IMAC Ni^{2+}-NTA	13	1070	3.0	358	179	73
(C) Lumβ4GalT-1 (6.2 g wet cell mass from 1 L culture)						
Crude extract	14	2300	172.9	13	1	100
IEX SP-sepharose	50	1919	19.0	101	7.6	83

Detection of the propeptide-natβ4GalT-1 fusion protein an immunoblot was accomplished by a polyclonal anti-β1,4-galactosyltransferase-β-galactosidase-fusionprotein-antibody from rabbit (kindly provided by Prof. E.G. Berger, Unversity of Zürich, Switzerland) and a polyclonal antibody anti-propeptide-lipase from rabbit (kindly provided by Prof. Dr. R. Freudl, Research Centre Jülich, Germany). Samples of protein fractions containing propeptide-natβ4GalT-1 were separated onto a 10% SDS-PAGE gel and subsequently blotted onto a PVDF membrane (BioRad, München, Germany). The membrane was blocked with 3% BSA in TBS buffer (10 mM Tris–HCl, 150 mM NaCl, pH 7.2). After a washing step with TBS buffer containing 0.1% Tween 20 the corresponding polyclonal antibody was applied for specific binding. After washing with TBS–Tween the blot was incubated with a second antibody, an anti-rabbit IgG alkaline phosphatase conjugate (Sigma Chemicals, St. Louis). For alkaline phosphatase detection blots were incubated with 20 mL 100 mM Tris–HCl pH 9.5, containing 100 mM NaCl, 5 mM $MnCl_2$, 66 μL NBT and 66 μL BCIP. The colouring reaction was stopped by adding 100 mM Tris–HCl pH 6.5, 100 mM EDTA.

Detection of the His_6propeptide-catβ4GalT-1 was also done by an immunoblot using a specific anti-His_6-antibody. Samples of His_6propeptide-catβ4GalT-1 were separated on SDS-PAGE gels and transferred onto PVDF membranes by the NuPAGE® Western transfer protocol (BioRad, München, Germany). Membranes were blocked with 3% BSA in TBS buffer (10 mM Tris–HCl, 150 mM NaCl, pH 7.2). A monoclonal anti-His_6-antibody conjugated to horse radish peroxidase (HRP) (Roche Diagnostics, Mannheim, Germany) was used for specific binding. After a washing step with TBS buffer containing 0.1% Tween 20 the blots were incubated with DAB substrate (Roche Diagnostics, Mannheim, Germany) and the HRP reaction was stopped by removal of the solution and addition of distilled water.

3.6. Detection of protease activity

The PepTag™ Protease Assay system (Promega, Mannheim, Germany) was used for testing protease activity during enzyme purification.

3.7. pH optimum and metal ion dependency

The optimal pH of the different β4GalT1 constructs was determined by activity measurements in 50 mM citrate buffer (pH 5–6.8) or 50 mM HEPES–NaOH buffer (pH 6.8–8.2). The metal ions (1 mM) Mg^{2+}, Ca^{2+}, and Co^{2+} were also tested beside Mn^{2+} under standard assay conditions. All samples were analyzed by HPLC.

3.8. Kinetic data for GlcNAc, Bn-GlcNAc, and IgG

The kinetic constants were derived from initial rate analysis by variation of the concentration of one substrate in the photometric enzyme assay. GlcNAc, GlcNAcβ1-Bn, and IgG were tested as acceptor substrates. Kinetic data for UDP-Gal were obtained in combination with each tested acceptor substrate using the purified enzyme fractions as shown in Table 1. For GlcNAc concentrations between 0 mM and 50 mM at a constant concentration of 2.5 mM UDP-Gal were used. UDP-Gal was varied from 0 mM to 8 mM in the presence of 37.5 mM GlcNAc. Benzyl 2-acetamido-2-deoxy-β-D-glucopyranoside (Bn-GlcNAc) concentrations between 0 mM and 10 mM at a constant concentration of 2 mM UDP-Gal were tested. UDP-Gal was varied from 0 mM to 5 mM in the presence of 1.5 mM Bn-GlcNAc). Concentrations of reduced and blocked rat IgG were between 0 μM and 120 μM at a constant concentration of 0.5 mM UDP-Gal. Reduction of disulfide bonds and subsequent blocking by iodacetamide was performed as described by Liljeblad et al. [40]. UDP-Gal was varied from 0 mM to 5 mM in the presence of 10 μM rat IgG.

3.9. Kinetic data and conversion of pNP-GlcNAc

The kinetic constants for the acceptor substrate *p*-nitrophenyl 2-acetamido-2-deoxy-β-D-glucopyranoside (*p*NP-GlcNAc) were derived from initial rate analysis at a variable substrate concentration and subsequent analysis by HPLC. Enzyme solutions were incubated at 30 °C with 5 mM UDP-Gal, variable concentrations (0–5 mM) of *p*NP-GlcNAc in 100 mM HEPES–NaOH pH 7.2 containing 25 mM KCl, 1 mM DTT, 2 mM $MnCl_2$, and 0.5 U alkaline phosphatase. The reactions

were stopped by heating for 5 min at 95 °C. The centrifuged samples were analysed by HPLC using LiChrospher® 100 RP-18 5 μ column (125 mm × 4 mm, Merck, Germany) with an acetonitrile gradient at room temperature (flow rate 0.5 mL/min, 20 μL sample volume, detection at 205 nm and 254 nm).

Kinetic constants were calculated according to the appropriate kinetic equations by use of SigmaPlot 10 (SPSS Science Software GmbH, Erkrath, Germany). For comparison of the conversion of *p*NP-GlcNAc by the three enzyme constructs the activity assay were incubated with 2 mU enzyme solutions and analysed as described above.

3.10. N-Glycan analysis of native and galactosylated rat IgG by capillary electrophoresis

Enzymatic releases, APTS-labeling of native and galactosylated *N*-glycans from rat IgG were performed according to the ProteomeLab Carbohydrate Labeling and Analysis Kit (Beckman Coulter, Krefeld, Germany). Subsequent separation of labeled *N*-glycans was accomplished by capillary electrophoresis (CE) on a P/ACE MDQ apparatus with LIF detection from Beckman Coulter (Krefeld, Germany). Conditions were applied as reported by Knudson and Simonian [41].

3.11. Enzymatic release and labeling of N-glycans from native rat IgG

Three hundred micrograms of rat IgG were reduced as described. The solution was evaporated to dryness at 50 °C and subsequently re-suspended in a 45 μL 50 mM $NaPO_4$ buffer, pH 7.5, containing 0.1% SDS and 58 mM 2-mercaptoethanol. The sample was heated for 20 min at 37 °C. After cooling down to room temperature 5 μL of NP-40 non-ionic detergent were added. For enzymatic *N*-glycan release PNGaseF was used at a final concentration of 36.000 U/mL. Incubation time for enzymatic release was 14 h at 37 °C. The solution was dried at 60 °C and subsequently re-suspended by adding 2 μL of 1 M sodium cyanoborohydride in THF and 2 μL of 100 mM APTS in 15% acetic acid. The reaction mixture was incubated for 90 min at 60 °C and 46 μL of millipore H_2O were added prior to CE analysis.

3.12. Enzymatic release and labeling of galactosylated N-glycans from rat IgG

Three hundred micrograms of rat IgG were reduced as described. For transfer reactions with propeptide-natβ4Gal-T1 1.5 mg/mL IgG and 1.5 mM UDP-Gal were incubated at 37 °C in 25 mM HEPES, pH 7.4, containing 1 mM $MgCl_2$ and 0.1% (v/v) Triton X-100 and 50 mU/mL of propeptide-natβ4Gal-T1 in total volume of 200 μL. Transfer reactions were stopped after different time intervals by dialysis using ultrafiltration membrane caps (10 kD cutoff, Vivaspin 500, Sartorius-Vivascience, Göttingen). The samples were washed five-times with 500 μL buffer (50 mM Tris, 150 mM NaCl and 0.1% (v/v) Tween 20, pH 7.6) and centrifuged at 10,000 rpm and 4 °C. For all further steps the protocol described above was used.

Galactosylation of rat IgG was followed by calculation of the relative portion of the peak areas for G0 (agalactosyl-bi-antennary *N*-glycan), G1 (α1,6 arm-galactosylated bi-antennary *N*-glycan), G1′ (α1,3 arm-galactosylated bi-antennary *N*-glycan), and G2 (fully galactosylated bi-antennary *N*-glycan).

4. Results and discussion

4.1. Expression of the pre-propeptide-natβ4GalT-1

The plasmid pLGalTΔ38 was used for the active expression of the pre-propeptide-natβ4GalT-1 in the periplasm of *E. coli*. Specific activities of up to 10 mU/mg could be already reached without IPTG induction of the promoter. With IPTG, however, an expression rate of up to 30 mU/mg was obtained. The formation of inclusion bodies was not observed. With this enzyme construct we get an equally high specific activity for human β4GalT-1 expressed in *E. coli* in comparison to that for recombinant β4GalT-1 expressed in yeast [24]. Therefore, we assume that the pre-propeptide of the lipase of *S. hyicus* has a positive effect on the production of human β4GalT-1 by supporting the formation of the correct conformation of the protein.

Setting up a purification strategy for the fusion protein turned out to be difficult because binding experiments to Q-sepharose and SP-sepharose, typical for the propeptide and GalT part, respectively, failed. However; binding to Zn^{2+}-NTA-IMAC was successful due to the relative high proportion of histidines in the propeptide part of the fusion protein (Scheme 3). Therefore, a combination of IEX (Q-sepharose) and IMAC was chosen as described above. An enzyme pool of human β4GalT-1 was obtained without contaminating side activities and is thus suitable for further biocatalytic applications (Table 1A).

Immunoblot analysis of a SDS-PAGE gel with the specific polyclonal antibodies against the propeptide and GalT part, respectively, revealed a major protein band for the propeptide-natβ4GalT-1 fusion protein in the crude extract, the flow through fractions of IEX and IMAC as well as the elution fraction after IMAC (lanes 1, 2, 4, and 5 in Fig. 1A and B, respectively). However, the immunoblots also reveal that the fusion protein is cleaved during Zn^{2+}-NTA-IMAC (lane 6 in Fig. 1A and 1B, respectively). The resulting protein fragments are specifically detected by the antibodies indicating the corresponding propeptide (Fig. 1A, lane 6) and GalT part (Fig. 1B, lane 6). The calibration of the immunoblot using the standards between 20.8 kDa and 47.5 kDa (for a 12% SDS-PAGE gel) gives molecular masses similar to the calculated ones: 62.1 kDa (63.7 kDa calculated) for propeptide-natβ4GalT-1, 26.6 kDa (22.9 kDa calculated) for the propeptide part and 40.4 kDa for the β4GalT-1 part (40.8 kDa calculated). Fig. 1B (lanes 6 and 7) also reveals that most of the fusion protein is cleaved. N-Terminal microsequencing analysis of the GalT protein band was not successful due to heterogeneity of the N-terminus. The appearance of distinct protein fragments detected by specific antibodies suggests that the propeptide-natβ4GalT-1 could be cleaved at the described proteolytic cleavage site between the amino acids 76 and 77 of the human β4GalT-1 (Expasy server, P15291, and Scheme 2). The heterogeneity of isolated β4GalTs from milk

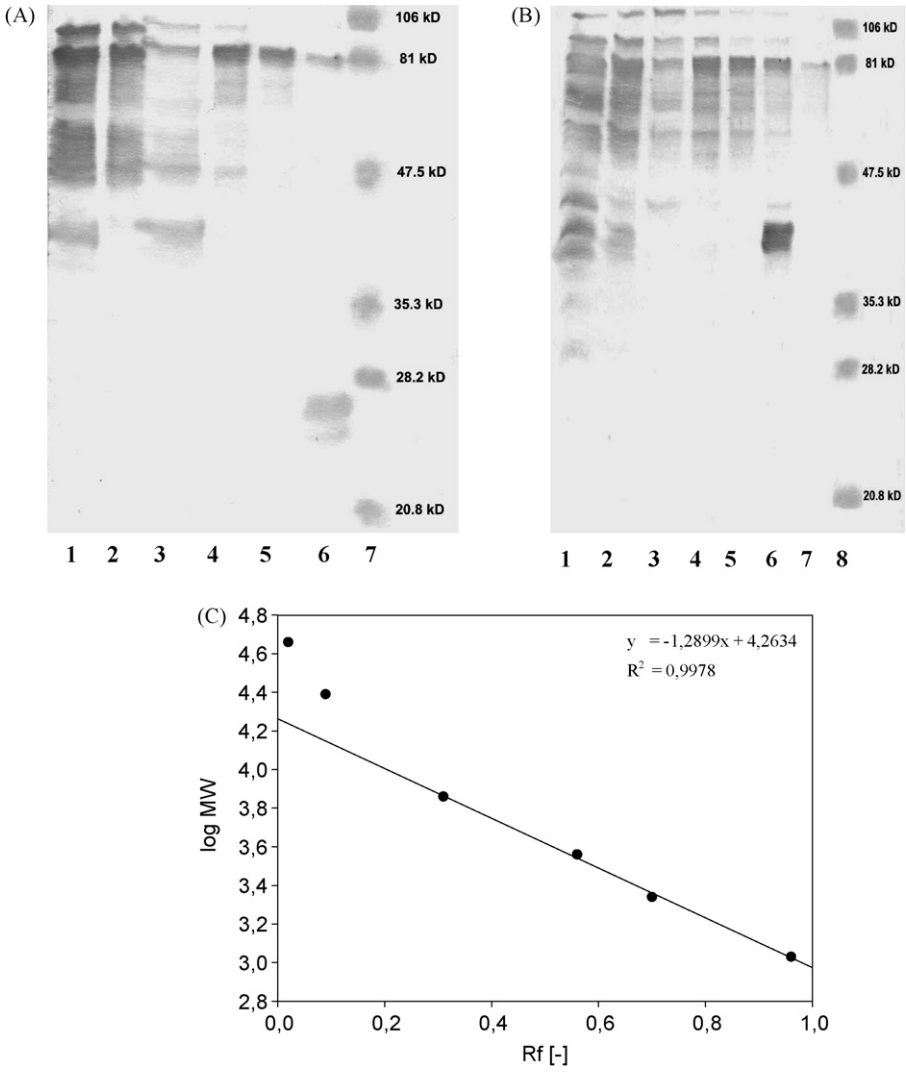

Fig. 1. Immunoblot analysis of propeptide-natβ4GalT-1 during purification. Samples of all steps of the purification were separated by SDS-PAGE (12% gels). After transfer of the separated protein bands the blots were incubated with a polyclonal antibody against the lipase of *Staphylococcus hyicus* (A) and a polyclonal anti-β-1,4-galactosyltransferase-β-galactosidase-fusionprotein-antibody from rabbit (B), respectively. Due to the 12% SDS-PAGE gel the standard proteins with molecular masses between 20.8 kD and 47.5 kD were used for calibration (C) and calculation of the molecular masses of the protein bands. (A) Lane1 crude extract; lane 2 IEX flow through; lane 3 IEX elution; lane 4 IMAC flow through; lanes 5 and 6 IMAC elution; lane 7 protein standard. (B) lane 1, crude extract; lane 2, IEX flow through; lane 3, IEX elution; lane 4, IMAC flow through; lanes 5–7, IMAC elution; lane 8, protein standard. Calculated molecular masses based on amino acid sequences (Scheme 3): propeptide-hβ4GalT-1: 67.2 kDa with 26.1 kDa for the propeptide and 41.1 kDa for β4GalT-1.

caused by proteolysis is well known and is attributed to multiple proteolytic cleavage sites in the stem region [4,42,43]. In our construct the presence of the stem region could cause the observed cleavage and the formation of a heterogeneous N-terminus. However, seven from 33 amino acids in the stem region are different in human β4GalT-1 when compared to the bovine enzyme (Scheme 2). Most importantly, protease activity in the crude extract and the enzyme fractions was not present suggesting that the observed cleavage is not caused by proteases (data not shown).

In addition, the cleavage products appear only during IMAC purification. Protein cleavage during IMAC is described in literature as catalyzed by divalent cations at specified peptide sequences [44,45]. According to the described sequence motifs a possible cleavage site in our enzyme construct could be in the sequence DKKPY at the C-terminus of the propeptide (Scheme 3), which is in accordance with the observed sizes of the cleavage products. We further confirmed that the observed cleavage of the propeptide-natβ4GalT-1 fusion protein during IMAC purification is reproducible.

4.2. Cloning and expression of the His_6propeptide-catβ4GalT-1 and lumβ4GalT-1

In order to eliminate the proposed cleavage site two strategies were pursued. First, we constructed a fusion protein containing the propeptide part, deleted by the five C-terminal amino acids DKKPY, and the catalytic domain of β4GalT-1 (Scheme 3). An N-terminal sixfold histidine tag was added to facilitate purification (His_6propeptide-catβ4GalT-1). With the expression vector

pET16b the resulting fusion protein was produced in the cytoplasm of *E. coli*. A specific activity of 2 mU/mg was reached which is in the range of described activities for periplasmic expression of human β4GalT-1 in *E. coli* [18]. Purification by Ni^{2+}-NTA-IMAC resulted in a preparation of His_6propeptide-catβ4GalT-1 which is suitable for further characterisation and biocatalytic applications (Table 1B). The occurrence of cleavage products of the enzyme construct was not observed.

Secondly, the luminal part of β4GalT-1 including the stem region and the catalytical domain was constructed and expressed in the periplasm of *E. coli* (Scheme 3). A specific activity of up to 13 mU/mg for the crude extract was obtained which is approximately 5–6 times higher when compared to data for the expression of the minimal catalytic domain [18]. The purification could be simplified by using SP-sepharose as a one-step-strategy. The resulting enzyme pool was free from contaminating side activities and was used for further applications (Table 1C).

4.3. Comparative biochemical characterisation

Significant differences were detected for the pH optimum of the different enzyme constructs (data not shown): pH 8 was found for propeptide-natβ4GalT-1, pH 7.6 for His_6propeptide-catβ4GalT-1, and pH 6.8 for lumβ4GalT1. In addition, the lumβ4GalT1 showed a rather broad pH activity profile (data not shown). We concluded that the observed differences of the pH optima are related to the additional components of the recombinant proteins carrying the same catalytic domain (Scheme 3). All further experiments were done at the specific optimal pH of each β4GalT-1 construct.

To ensure that comparative characterisation of kinetics are performed under optimal conditions the metal ion dependency of all three β4GalT-1 constructs were examined. They showed the highest activity with 1 mM $MnCl_2$, but each construct also individually tolerated other metal ions (Fig. 2). The propeptide-natβ4GalT-1 accepted also Mg^{2+} (15% residual activity), whereas lumβ4GalT1 was also active with Co^{2+}-ions (18% residual activity). In contrast, His_6propeptide-catβ4GalT-1 was not that flexible and showed relative low residual activities with Mg^{2+} and Ca^{2+} (5% each). As expected, without metal ions all three constructs were not active. The importance of Mn^{2+} as a cofactor for β4GalT-1 was described before for the human [46] and bovine enzyme [47]. The recombinant minimal catalytic domain of the bovine β4GalT-1 showed low activity in the presence of Co^{2+} [47]. In conclusion, we may also deduce from our results that each β4GalT-1 construct exhibit distinct characteristics for their metal ion dependent activity.

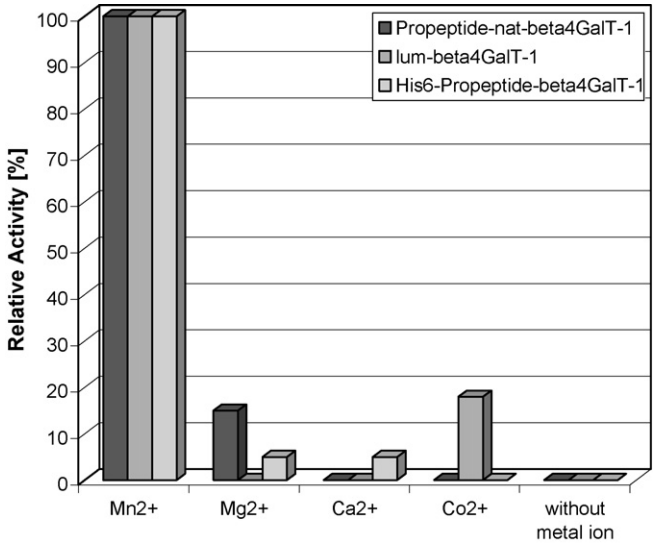

Fig. 2. Metal ion dependency of the different β4GalT-1 constructs. Experiments were performed as described in Section 2.

4.4. Comparative kinetic characterisation and biocatalytic conversions

The kinetic characterization of the β4GalT-1 constructs revealed distinct properties for each of the tested acceptor substrates (Table 2). When compared to GlcNAc all enzymes showed significantly increased catalytic efficiencies ($V_{max\ app}/K_{m\ app}$) with Bn-GlcNAc and *p*NP-GlcNAc, respectively. A closer look at reaction velocities ($V_{max\ app}$) reveals that Bn-GlcNAc is the favourite substrate for propeptide-natβ4GalT-1 (sevenfold increase, Table 2B) and *p*NP-GlcNAc is preferred by His_6propeptide-catβ4GalT-1 (21-fold increase, Table 2C). In addition, both enzymes exhibit increased affinities for the glycoside acceptors. In comparison to lumβ4GalT-1 the increase of catalytic efficiencies is significant higher suggesting that propeptide-natβ4GalT-1 and His_6propeptide-catβ4GalT-1 are more suitable for the conversion of hydrophobic glycosides (Table 2A–C). The fact that hydrophobic aglycones lower the K_m for acceptor substrates is known for β4GalT. A recent study on the acceptor specificity of the enzyme from bovine milk emphasizes the importance of a hydrophobic aglycone for the binding to the active site of the enzyme [15]. Our data also confirm the observation that substrate inhibition occurs more frequently with hydrophobic acceptor glycosides (Table 2A–C). However, the comparison with bovine milk β4GalT with the propeptide-natβ4GalT-1 and His_6propeptide-catβ4GalT-1, respectively, reveals that the improvement for our enzyme constructs is due to a significant increase in activity. We achieve much higher improvements in catalytic efficiencies when changing the acceptor substrate from GlcNAc to Bn-GlcNAc and *p*NP-GlcNAc. Whereas the bovine milk β4GalT shows only a fivefold increase [15] due to higher enzyme affinities, the catalytic efficiency for Bn-GlcNAc and for *p*NP-GlcNAc increases 67-fold and 27-fold with our enzyme constructs propeptide-natβ4GalT-1 and His_6propeptide-catβ4GalT-1, respectively, due to higher activities. We conclude that the catalytic efficiency of β4GalT-1 for hydrophobic aglycons can be significantly further improved by our enzyme constructs. This is especially emphasized by comparing our enzyme constructs for their conversion of *p*NP-GlcNAc (Fig. 3). This acceptor was selected since the nitro-group can be reduced to an amino-functionality for attachment onto biomaterial surfaces. With His_6propeptide-catβ4GalT-1 quantitative conversion of *p*NP-GlcNAc is already reached after 2 h. The propeptide-natβ4GalT-1 and the lumβ4GalT-1,

Table 2
Kinetic characterization of β4GalT-1 constructs

	UDP-Gal				GlcNAc			
	$V_{max\ app}$ (mU/mg)	$K_{m\ app}$ (mM)	$K_{iS\ app}$ (mM)	$V_{max\ app}/K_{m\ app} \times 10^{-3}$	$V_{max\ app}$ (mU/mg)	$K_{m\ app}$ (mM)	$K_{iS\ app}$ (mM)	$V_{max\ app}/K_{m\ app} \times 10^{-3}$
(A) GlcNAc as acceptor								
Propeptide-natβ4GalT-1	106.7 ± 3.7	0.21 ± 0.4	12.06 ± 0.4	0.51	158.7 ± 8.7	4.20 ± 0.80	–	0.04
His_6-propeptide-catβ4GalT-1	254.4 ± 6.8	0.37 ± 0.1	8.6 ± 0.1	0.69	234.8 ± 7.5	2.28 ± 0.30	–	0.10
Lumβ4GalT-1	60.3 ± 4.5	0.21 ± 0.4	12.0 ± 0.4	0.29	55.2 ± 1.7	5.50 ± 12.10	264 ± 12.1	0.01
	UDP-Gal				GlcNAcβ1-Bn			
	$V_{max\ app}$ (mU/mg)	$K_{m\ app}$ (mM)	$K_{iS\ app}$ (mM)	$V_{max\ app}/K_{m\ app} \times 10^{-3}$	$V_{max\ app}$ (mU/mg)	$K_{m\ app}$ (mM)	$K_{iS\ app}$ (mM)	$V_{max\ app}/K_{m\ app} \times 10^{-3}$
(B) Bn-GlcNAc as acceptor								
Propeptide-natβ4GalT-1	1138.2 ± 42.3	0.2 ± 0.04	–	5.69	1067.8 ± 29.9	0.40 ± 0.20	8.10 ± 0.20	2.67
His_6propeptide-catβ4GalT-1	418.4 ± 7.9	0.5 ± 0.2	7.2 ± 0.2	0.84	339.0 ± 17.5	0.20 ± 0.20	8.10 ± 0.20	1.70
Lumβ4GalT-1	168.3 ± 8.7	1.1 ± 0.2	–	0.15	217.3 ± 4.7	0.20 ± 0.20	17.50 ± 0.20	1.09
	UDP-Gal				GlcNAcβ1-*P*np			
	$V_{max\ app}$ (mU/mg)	$K_{m\ app}$ (mM)	$K_{iS\ app}$ (mM)	$V_{max\ app}/K_{m\ app} \times 10^{-3}$	$V_{max\ app}$ (mU/mg)	$K_{m\ app}$ (mM)	$K_{iS\ app}$ (mM)	$V_{max\ app}/K_{m\ app} \times 10^{-3}$
(C) *p*NP-GlcNAc as acceptor								
Propeptide-natβ4GalT-1	n.d.	n.d.	n.d.	n.d.	380.0 ± 94	0.84 ± 0.334	2.51 ± 1.14	0.45
His_6propeptide-catβ4GalT-1	1409.4 ± 58.5	2.1 ± 0.25	-	0.67	4931.0 ± 506	1.82 ± 0.25	1.66 ± 0.25	2.71
Lumβ4GalT-1	n.d.	n.d.	n.d.	n.d.	157.0 ± 41	0.95 ± 0.385	3.80 ± 2.47	0.17
	UDP-Gal				IgG			
	$V_{max\ app}$ (mU/mg)	$K_{m\ app}$ (mM)	$K_{iS\ app}$ (mM)	$V_{max\ app}/K_{M\ app} \times 10^{-3}$	$V_{max\ app}$ (mU/mg)	$K_{m\ app}$ (μM)	$K_{iS\ app}$ (μM)	$V_{max\ app}/K_{m\ app}$[a] $\times 10^{-3}$
(D) Rat IgG as acceptor								
Propeptide-natβ4GalT-1	156.3 ± 3.8	0.1 ± 0.02	–	1.56	154.6 ± 3.5	1.9 ± 0.5	42.5 ± 0.5	81.4
His_6propeptide-catβ4GalT-1	177.7 ± 10.3	0.07 ± 0.07	1.6 ± 0.07	2.53	138.2 ± 9.2	21.07 ± 2.9	130.6 ± 2.9	6.6
Lumβ4GalT-1	174.1 ± 20.5	0.4 ± 0.1	1.5 ± 0.1	0.43	178.4 ± 7.1	10.7 ± 2.1	159.2 ± 2.1	16.7

n.d.: not determined; –: no substrate inhibition.
[a] $K_{m\ app}$ value in mM.

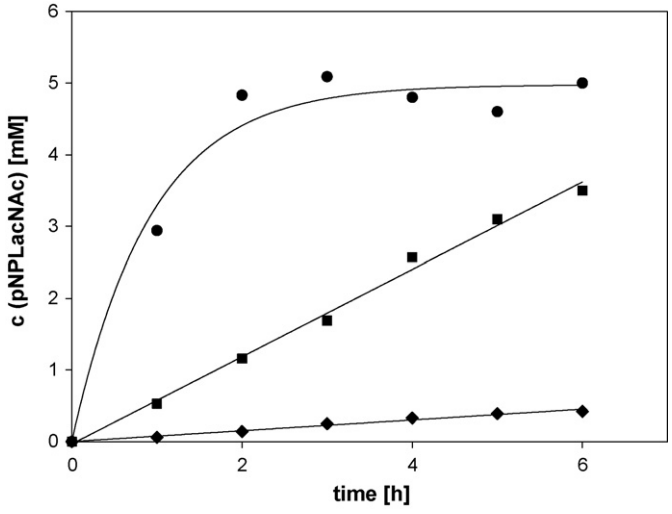

Fig. 3. Conversion of *p*NP-GlcNAc by different β4GalT-1 constructs. (●) His_6propeptide-catβ4GalT-1, (♦) propeptide-natβ4GalT-1, (■) lumβ4GalT-1. Experiments were performed as described in Section 2.

however, show only 70% and 10% conversion of *p*NP-GlcNAc, respectively, after 6 h. We conclude that the His_6propeptide-catβ4GalT-1 with the fused propeptide is especially useful for the conversion of GlcNAc glycosides carrying a hydrophobic aglycone whereas the propeptide-natβ4GalT-1 is less efficient due to the loss of the propeptide during IMAC purification. The higher conversion rate of the latter in comparison to lumβ4GalT-1 may be attributed to the residual part of the membrane anchor of β4GalT-1.

In order to investigate biocatalytic differences towards more complex substrates immunoglobulin G from rat was selected as glycoprotein acceptor substrate since it contains bi-antennary agalactosyl- (G0 and G1) and galactosyl-*N*-glycans (G2) at a single site (Asn297) of the heavy chains (Scheme 1B) [48]. The reduction of the disulphide bridges of IgG should facilitate the accessibility of the N-glycans for the galactosyltransferases. All three enzymes showed similar $V_{max\ app}$ values for IgG and UDP-Gal (Table 2D). However, propeptide-natβ4GalT-1 has the best catalytic efficiency which is mainly due to a relative high affinity when compared to lumβ4GalT-1 and His_6propeptide-catβ4GalT-1. Human serum IgG was recently shown to be efficiently galactosylated with recombinant bovine β4GalT-1 [49] and β4GalT from *H. pylori* [50]. However, kinetic data

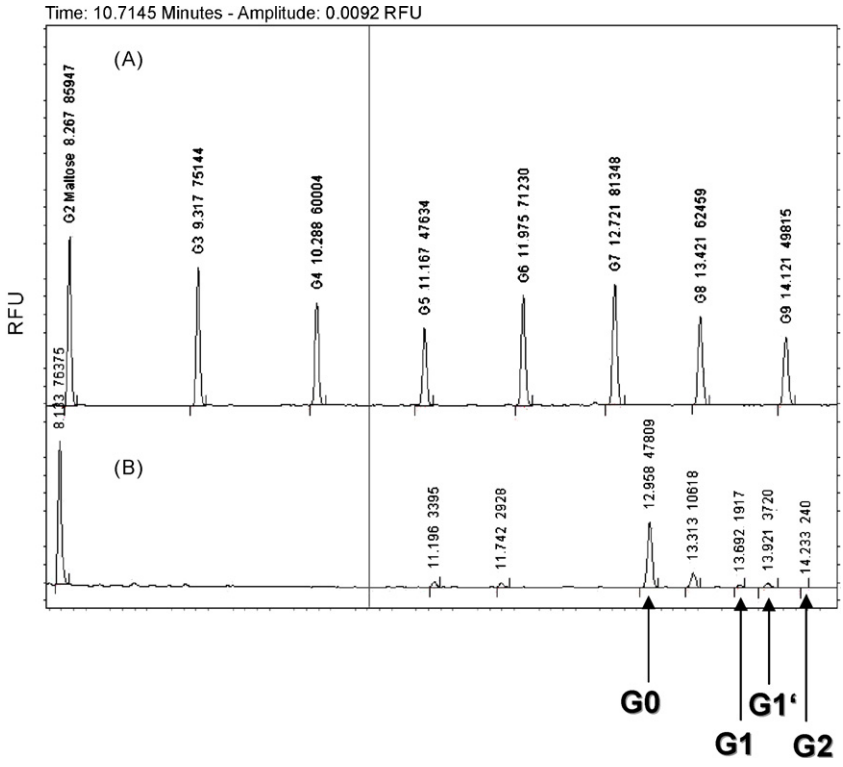

Fig. 4. Electropherograms of APTS-derivatized standard glucose ladder (A) and APTS-derivatized *N*-glycans (B) released by PNGase F from rat IgG. Peaks were annotated as proposed by Knudson and Simonian [41].

for IgG were not presented by these authors. Most interestingly, the affinities of our constructs for IgG are in the μM-range whereas the K_m values for the isolated G0, G1′ and G1 *N*-glycan structures from IgG are in the mM-range for rat liver β4GalT-1 [51].

In order to demonstrate galactosylation of rat IgG by propeptide-natβ4GalT-1, the *N*-glycans were released after enzymatic galactose transfer by PNGase F and APTS-labeled *N*-glycans were subsequently analysed by separation on CE [41]. Fig. 4 depicts the constitution of bi-antennary *N*-glycans on rat IgG with the agalacto-antennae (G0), the α1,6 arm-galactosylated bi-antennary *N*-glycan (G1), and the α1,3 arm-galactosylated bi-antennary *N*-glycan (G1′). The relative peak areas account for 74.3% (G0), 3.0% (G1), 5.8% (G1′), and 0.3% (G2) (Fig. 5). After 2 h incubation with propeptide-natβ4GalT-1 G1′ (35.2%) accumulates as the predominating structure. However, since G2 has simultaneously been formed with a relative peak area of 24.7% and G1 only increases to 9.5% we conclude that G2 is formed via formation of G1. Additional support comes from the time course of the G1 and G1′ structure, respectively. The relative peak area for G1 decreases faster than that for G1′. After 64 h incubation time conversion of G0–G2 (93%) is almost quantitative with G1′ (7%) remaining. Kinetic parameters for the formation of G1 or G1′ cannot be determined from our studies. With recombinant bovine β4GalT-1 acting on human serum IgG it was found that the conversion of G0–G1 and G1′ occurs very rapidly, whereas the conversion from G1–G2 is very slow [49]. However, G1 was not distinguished from G1′ by HPLC-analysis in this study. In a more

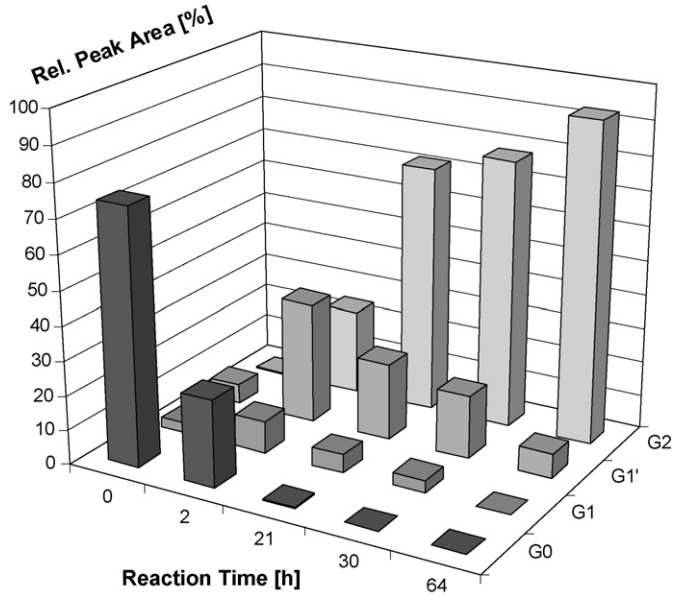

Fig. 5. Enzymatic galactosylation of rat IgG and subsequent CE-analysis of the APTS-derivatized *N*-glycans released by PNGase F. The relative peak areas in the electropherograms for the *N*-glycans structures after the indicated incubation time with propeptide-natβ4GalT-1 are given. G0 (agalactosyl-bi-antennary *N*-glycans), G1 (α1,6 arm-galactosylated bi-antennary *N*-glycans), G1′ (α1,3 arm-galactosylated bi-antennary *N*-glycans), and G2 (fully galactosylated bi-antennary *N*-glycans).

detailed work, Ramasamy et al. concluded that human β4GalT-1 prefers the α6-antenna forming G1 at lower concentrations of the bi-antennary *N*-glycan structure [8]. At a higher concentration the α3-antenna is the preferred substrate and G1′ is formed [8,51]. In our studies G0 as the predominating bi-antennary *N*-glycan structure of rat IgG provides a relative high concentration for the formation of each of these substrates (Fig. 5). We conclude that G1′ is preferentially formed and accumulates because G1′ provides the α1,6-antenna substrate which inhibits the enzyme at higher concentrations [8] (Scheme 1B). The following decrease of the G0 concentration fosters the formation of G1 which provides the α1,3-antenna as substrate for the formation of G2.

5. Conclusions and future applications

Our studies demonstrate the impact of the fusion protein on the biocatalytic properties of human β4GalT-1 expressed in *E. coli*. Biocatalysts are now available with high catalytic activities towards hydrophobic GlcNAc acceptor glycosides. In this respect, our novel enzyme constructs should be also suitable for the conversion of glycolipids. Currently, work is in progress in our group to utilize the His_6propeptide-β4GalT-1 for the production of chemically modified LacNAc structures, to use them for further enzymatic modifications, and to immobilize them onto biomaterial surfaces. Concerning the propeptide-natβ4GalT-1 this enzyme is suitable for the re-glycosylation of glycoproteins.

Acknowledgements

L.E. acknowledges financial support by the DFG through the Research Training Group 1035 “Biointerface” (grant for B.S.) and the projects EL-1035/6-1 and EL-1035/6-2. L.E. and V.K. also acknowledge financial support for a bilateral DAAD-AVCR project PPP-D7-CZ 26/04–05D/03/44448 and No. IAA400200503 as well as LC06010 from GAAVCR (V.K). We thank Prof. Dr. R. Freudl and Dr. M. Klein (Institute for Biotechnology 1, Research Center Jülich) for providing the pLGalTΔ38 vector and anti-propeptide antibody. We also thank Prof. Dr. E.G. Berger (Institute of Physiology, University of Zürich) for providing the anti-GalT antibody. The authors acknowledge ESF project COST Chemistry providing travel funds, D25/001/01.

References

[1] N.L. Shaper, J.H. Shaper, in: T. Taniguchi, K. Honke, M. Fukuda (Eds.), Handbook of Glycosltransferases and Related Genes, Springer, Tokyo, 2002, pp. 11–19.
[2] K. Furukawa, H. Clausen, in: T. Taniguchi, K. Honke, M. Fukuda (Eds.), Handbook of Glycosltransferases and Related Genes, Springer, Tokyo, 2002, pp. 20–26.
[3] N.L. Shaper, M. Charron, N.-W. Lo, J.H. Shaper, J. Mamm. Gland Biol. Neoplasia 3 (1998) 315–324.
[4] E.G. Berger, J. Rohrer, Biochimie 85 (2003) 261–274.
[5] L.N. Gastinel, C. Cambillau, Y. Bourne, EMBO J. 18 (1999) 3546–3557.
[6] B. Ramakrishnan, E.E. Boeggeman, V. Ramasamy, P.K. Qasba, Curr. Opin. Struct. Biol. 14 (2004) 593–600.
[7] P.K. Qasba, B. Ramakrishnan, E. Boeggeman, Trends Biochem. Sci. 30 (2005) 53–62.
[8] V. Ramasamy, B. Ramakrishnan, E. Boeggeman, D.M. Ratner, P.H. Seeberger, P.K. Qasba, J. Mol. Biol. 353 (2005) 53–67.
[9] G. D’Agostaro, B. Bendiak, M. Tropak, Eur. J. Biochem. 183 (1989) 211–217.
[10] T. Uejima, M. Uemura, S. Nozawa, H. Narimatsu, Cancer Res. 52 (1992) 6158–6163.
[11] K.A. Masri, H.E. Appert, M.N. Fukuda, Biochem. Biophys. Res. Commun. 157 (1988) 657–663.
[12] C.-H. Wong, G.M. Whitesides (Eds.), Enzymes in Synthetic Organic Chemistry, Elsevier Science, Oxford, 1994, pp. 252–311.
[13] A. Zervosen, L. Elling, J. Am. Chem. Soc. 118 (1996) 1836–1840.
[14] Y. Nishida, H. Tamakoshi, Y. Kitagawa, K. Kobayashi, J. Thiem, Angew. Chem. Int. Ed. Engl. 39 (2000) 2000–2003.
[15] I. Brockhausen, M. Benn, S. Bhat, S. Marone, J.G. Riley, P. Montoya-Peleaz, J.Z. Vlahakis, H. Paulsen, J.S. Schutzbach, W.A. Szarek, Glycoconj. J. 23 (2006) 525–541.
[16] E.E. Boeggeman, B. Ramakrishnan, P.K. Qasba, Protein Exp. Purif. 30 (2003) 219–229.
[17] M. Malissard, L. Borsig, S. Di Marco, M.G. Grütter, U. Kragl, C. Wandrey, E.G. Berger, Eur. J. Biochem. 239 (1996) 340–348.
[18] M. Malissard, E.G. Berger, Eur. J. Biochem. 268 (2001) 4352–4358.
[19] R. Wohlgemuth, CHIMIA 59 (2005) 735–740.
[20] E.E. Boeggeman, P. Balaji, N. Sethi, A. Masibay, P. Qasba, Protein Eng. 6 (1993) 779–785.
[21] Y. Wang, S.S. Wong, M.N. Fukuda, H. Zu, Z. Liu, Q. Tang, H.E. Appert, Biochem. Biophys. Res. Commun. 204 (1994) 701–709.
[22] S. Shibatani, K. Fujiyama, S. Nishiguchi, T. Seki, Y. Maekawa, J. Biosci. Bioeng. 91 (2001) 85–87.
[23] Y. Zhang, V. Malinovskii, T. Fiedler, K. Brew, Glycobiology 9 (1999) 815–822.
[24] M. Malissard, S. Zeng, E.G. Berger, Glycoconj. J. 16 (1999) 125–139.
[25] M. Malissard, S. Zeng, E.G. Berger, Biochem. Biophys. Res. Commun. 267 (2000) 169–173.
[26] C.-H. Wong, Y. Ichikawa, T. Krach, C. Gautheron-Le Narvor, D.P. Dumas, G.C. Look, J. Am. Chem. Soc. 113 (1991) 8137–8145.
[27] X. Qian, K. Sujino, M.M. Palcic, Carbohydrates in chemistry and biology. Part I. Chemistry of saccharides, in: B. Ernst, G.W. Hart, P. Sinay (Eds.), Enzymatic Synthesis of Glycosides and Carbohydrate–Receptor Interaction, vol. 2, Wiley–VCH, Weinheim, 2000, pp. 685–703.
[28] F. Götz, F. Popp, E. Korn, K.H. Schleifer, Nucleic Acid Res. 13 (1985) 5895–5906.
[29] W. Liebl, F. Götz, Mol. Gen. Genet. 204 (1986) 166–173.
[30] J. Meens, M. Herbort, M. Klein, R. Freudl, Appl. Environ. Microbiol. 63 (1997) 2814–2820.
[31] D. Horton, Org. Synth. Coll. 46 (1966).
[32] D. Horton, Org. Synth. Coll. 5 (1973).
[33] J.E. Heidlas, W.J. Lees, P. Pale, G.M. Whitesides, J. Org. Chem. 57 (1992) 146–151.
[34] S. Singh, J. Packwood, C.J. Samuel, P. Critchley, D.H. Crout, Carbohydr. Res. 279 (1995) 293–306.
[35] R. Roy, F.D. Tropper, T. Kortison, J. Boratynski, J. Chem. Soc., Chem. Commun. 7 (1991) 536–538.
[36] B. Coxon, Carbohydr. Res. 340 (2005) 1714–1721.
[37] R. Higuchi, B. Krummel, R.K. Saiki, Nucleic Acids Res. 16 (1988) 7351–7367.
[38] M.M. Bradford, Anal. Biochem. 72 (1976) 248–254.
[39] D.H.P. Barratt, L. Barber, N.J. Kruger, A.M. Smith, T.L. Wang, C. Martin, Plant Physiol. 127 (2001) 655–664.
[40] M. Liljeblad, A. Lundblad, P. Pahlsson, Glycoconj. J. 17 (2000) 323–329.
[41] V.F. Knudson, M.H. Simonian, PACE Setter 9 (2005) 1–4 (www.beckmancoulter.com/Literature/BioResearch/NL-9953A.pdf).
[42] S.C. Magee, R. Mawal, K.E. Ebner, Biochemistry 13 (1974) 99–102.
[43] J.P. Prieels, E. Maes, M. Dolmans, J. Leonis, Eur. J. Biochem. 60 (1975) 525–531.
[44] R. Krishnamurthy, R.D. Madurawe, K.D. Bush, J.A. Lumpkin, Biotechnol. Prog. 11 (1995) 643–650.

[45] D.P. Humphreys, B.J. Smith, L.M. King, S.M. West, D.G. Reeks, P.E. Stephens, Protein Eng. 12 (1999) 179–184.
[46] M. Amado, R. Almeida, T. Schwientek, H. Clausen, Biochim. Biophys. Acta: Gen. Subjects 1473 (1999) 35–53.
[47] E. Boeggeman, P.K. Qasba, Glycobiology 12 (2002) 395–407.
[48] T.S. Raju, J.B. Briggs, S.M. Borge, A.J.S. Jones, Glycobiology 10 (2000) 477– 486.
[49] D. Warnock, X. Bai, K. Autote, J. Gonzales, K. Kinealy, B. Yan, J. Qian, T. Stevenson, D. Zopf, R.J. Bayer, Biotechnol. Bioeng. 92 (2005) 831–842.
[50] S.-W. Chung, H.-S. Joo, K.-S. Jang, H.-J. Lee, S.-G. Lee, B.-G. Kim, Enzyme Microb. Technol. 39 (2006) 60–66.
[51] M. Paquet, S. Narasimhan, H. Schachter, M. Moscarello, J. Biol. Chem. 259 (1984) 4716–4721.
[52] G. Watzele, E.G. Berger, Nucleic Acid Res. 18 (1990) 7174.